Liquid Crystals
Publication details, including instructions for authors and subscription information:
http://www.informaworld.com/smpp/title~content=t713926090

Orientational order and dynamics of fluorescent probes in aligned lyotropic phases by fluorescence depolarization spectroscopy. Perylene in a nematic discotic phase. A comparison with ^{2}H NMR

D. Catalano[a]; A. Lenzi[a]; C. A. Veracini[a]
[a] Dipartimento di Chimica e Chimica Industriale, Università di Pisa, Pisa, Italy

To cite this Article Catalano, D. , Lenzi, A. and Veracini, C. A.(1993) 'Orientational order and dynamics of fluorescent probes in aligned lyotropic phases by fluorescence depolarization spectroscopy. Perylene in a nematic discotic phase. A comparison with ^{2}H NMR', Liquid Crystals, 14: 5, 1457 — 1468

To link to this Article: DOI: 10.1080/02678299308026458

URL: http://dx.doi.org/10.1080/02678299308026458

LIQUID CRYSTALS, 1993, VOL. 14, NO. 5, 1457–1468

Orientational order and dynamics of fluorescent probes in aligned lyotropic phases by fluorescence depolarization spectroscopy. Perylene in a nematic discotic phase

A comparison with ^{2}H NMR

by D. CATALANO, A. LENZI and C. A. VERACINI*
Dipartimento di Chimica e Chimica Industriale, Università di Pisa,
via Risorgimento 35, 56100 Pisa, Italy

The orientational order and dynamics of perylene in the nematic discotic phase (N_dII) of the potassium laurate/KCl/decanol/water system has been investigated by fluorescence depolarization (FD) spectroscopy. The order parameters of perylene-d_{12} in the same phase had been previously determined by ^{2}H NMR. FD experiments were performed with the phase-modulation technique in the temperature range between 10°C and 50°C. At each temperature we could determine $\langle P_2 \rangle$ and $\langle P_4 \rangle$ for the axis of the transition moments of perylene, together with the rotational correlation time Θ_R. All these quantities assume reasonable values and show regular trends as functions of temperature. In particular, $\langle P_2 \rangle$ is in good agreement with that determined by ^{2}H NMR.

1. Introduction

The orientational order of aromatic polycyclic hydrocarbons in lyotropic and thermotropic liquid crystals, as well as in membranes, has been studied by various spectroscopic techniques such as electron spin resonance [1], linear dichroism [2], fluorescence depolarization [3] and deuterium nuclear magnetic resonance (^{2}H NMR) [4–6]. We will compare, in particular, the merits and difficulties of the two latter techniques which appear to be complementary in many aspects. Fluorescence depolarization, FD, can be measured either by following the decaying response to a pulse excitation or by means of phase techniques [7]. FD data give access to high order orientational parameters [8] ($\langle P_4 \rangle$ can be determined together with $\langle P_2 \rangle$), but, as for other optical techniques, only the order parameters relative to the axes of the transition moments can be determined. Moreover, the dynamics of the system to be investigated are accessible in the form of correlation times, but the analysis of FD data is quite complex [9]. ^{2}H NMR spectroscopy, through measurements of the quadrupolar splittings, is a very powerful technique for the determination of the ordering matrix of probes oriented in aligned samples. For biaxial molecules, for instance, two independent order parameters, the principal one $\langle D^2_{00} \rangle$, and the order biaxiality $\langle D^2_{02} \rangle$, can be simultaneously investigated [6]; on the other hand, the obtainable information is limited to the second rank order parameters. The relationships between quadrupolar or dipolar splittings and the order parameters are very simple; moreover, the possible coexistence of multiple phases can be straightforwardly revealed. These facilities, however, are counterbalanced by the relatively low intrinsic sensitivity of NMR

---

*Author for correspondence.

spectroscopy, which requires a substantial amount of dissolved probe in order to detect the spectrum in reasonable time. This may perturb and modify the mesophase.

In the present paper we report the study of the orientational order of perylene in a nematic lyotropic mesophase of discotic type (N_dII) by FD spectroscopy. The results are compared with those yielded by ^{2}H NMR.

2. Materials and methods

The lyotropic discotic phase studied is the one described by Long Jr. [10]. The composition adopted was 31·89 per cent potassium laurate (synthesized from lauric acid according to the procedure of Saupe [11], 6·39 per cent 1-decanol, 4·25 per cent KCl and 57·46 per cent H_2O. The discotic nematic phase occurs between 10°C and 63°C [6, 10]. The components were mixed in a glass tube containing an amount of perylene, evaporated from ethanol, sufficient to obtain an absorbance of 0·2 at 409 nm when the lyotropic solution was introduced into a 0·5 mm optical path length cuvette. The concentration of perylene in the final solution was $1{\cdot}3 \times 10^{-4}$ M. Perylene (Aldrich 'Gold Marke') was used without purification. The tube was sealed and the mixture mechanically shaken for 12 h. After obtaining a homogeneous solution, the sample was left undisturbed for 2 days.

The liquid crystal so prepared was put into a 0·5 mm thick quartz cuvette and left for 3 days in a 2000 G magnetic field parallel to the layer of solution, as shown in figure 1. In these conditions a macroscopic orientation of the phase is reached in which the phase director is perpendicular to the wider surface of the cuvette. The orienting effect of the cuvette walls then preserves the homogeneous alignment of the sample out of the magnetic field for several days. This was verified by observing the sample through cross polarizers: a homogeneous dark pattern of the transmitted light was found. Moreover, the stability of the alignment was confirmed by the constant value of the static fluorescence polarization during each series of measurements. The degree of order of the sample could be varied by systematically varying its temperature at least between 10°C and 40°C, as we will see later. Of course, the chosen thickness of the cuvette is critical for obtaining this kind of behaviour of the macroscopic order of the phase.

Fluorescence depolarization measurements were performed using a GREG 200 Phase-modulation system (ISS inc. Urbana, Illinois) equipped with a 300 W xenon arc lamp. The wavelength of the exciting light was 409 nm (10 nm band-pass) corresponding to a maximum in the vibrational structure of the $S_0 \rightarrow S_1$ electronic transition band of perylene [12]. The light was linearly polarized along the Z axis of the laboratory frame (see figure 2). The emission from perylene was monitored by measuring the polarized emission along the Z and X axes through a 450 nm cut-off filter in order to

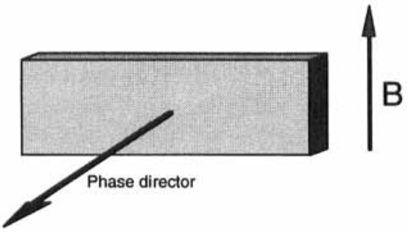

Figure 1. Cuvette setting in the magnetic field. Sample thickness 0·5 mm, $B = 2000$ G, orientation period 48 h.

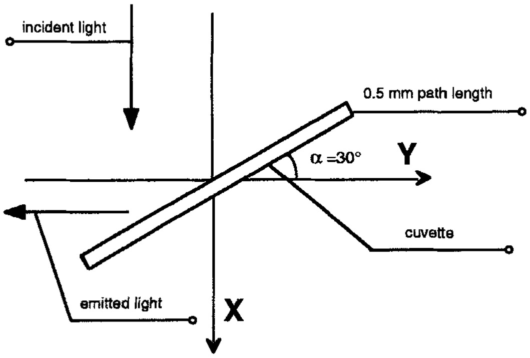

Figure 2. Cuvette setting in the fluorimeter. The reflected light is directed out of the photo-tube with an angle of 30° between the cuvette surface and the Y_{Lab} axis.

eliminate the scattered light. Modulation frequencies ranged from 10 to 210 MHz. Each final result for the phase shift and modulation ratio is the average of 60 measurements, each in turn produced after 40 instrumental samplings.

Special attention was given to the sample setting (see figure 2). In order to avoid the isotropic absorption of the incident light when the phase director lies along the X axis (the symmetry axis of the discotic phase is perpendicular to the wider surface of the cuvette) the sample was put into the fluorimeter with an angle of 30° between the cuvette surface and the Y axis; this setting also minimizes the reflected light falling on the emission phototube.

3. Theory and experimental data analysis

The phase modulation [13] technique allows the study of the dynamics of fluorescence depolarization by the use of intensity-modulated incident light, linearly polarized along the Z axis (see figure 2 for the definition of the reference frame). The phase shift and the modulation ratio between the light emitted with parallel (along the Z axis, $\parallel$) and perpendicular (along the Y axis, $\perp$) polarization are then detected. If the intensity of the incident light is modulated by a sinusoidal wave of frequency ω, the phase shift and the modulation ratio can be expressed according to the following expressions:

$$\Delta\phi(\omega)=\phi_{\perp}(\omega)-\phi_{\parallel}(\omega)=\arctan\left(\frac{S_{\perp}(\omega)C_{\parallel}(\omega)-S_{\parallel}(\omega)C_{\perp}(\omega)}{S_{\perp}(\omega)S_{\parallel}(\omega)+C_{\parallel}(\omega)C_{\perp}(\omega)}\right), \tag{1a}$$

$$M_{\mathrm{R}}(\omega)=\frac{M_{\perp}(\omega)}{M_{\parallel}(\omega)}=\sqrt{\left(\frac{S_{\perp}^{2}(\omega)+C_{\perp}^{2}(\omega)}{S_{\parallel}^{2}(\omega)+C_{\parallel}^{2}(\omega)}\right)\frac{\Gamma_{\parallel}(\omega)}{\Gamma_{\perp}(\omega)}}, \tag{1b}$$

where $C_{\lambda}(\omega)$, $S_{\lambda}(\omega)$ and $\Gamma_{\lambda}(\omega)$, respectively, are given by

$$C_{\lambda}(\omega)=\int_{0}^{\infty}dtI_{\mathrm{em}}^{\lambda}(t)\cos(\omega t), \tag{2a}$$

$$S_{\lambda}(\omega)=\int_{0}^{\infty}dtI_{\mathrm{em}}^{\lambda}(t)\sin(\omega t); \qquad \lambda=\parallel,\perp \tag{2b}$$

$$\Gamma_{\lambda}(\omega)=\int_{0}^{\infty}dtI_{\mathrm{em}}^{\lambda}(t). \tag{2c}$$

$I^{\lambda}_{\mathrm{em}}(t)$ is the function of time which describes the emission of light with λ polarization after a pulsed excitation.

Explicit expressions for $I^{\lambda}_{\mathrm{em}}(t)$ have been given by Weber [14], Szabo [15], and Zannoni [16]. The last author has developed suitable expressions for liquid crystalline systems, and, in particular, lyotropic aggregates of various shapes and symmetry, such as spherical micelles, lamellae, infinite cylinders.

The fluorescence intensity $I^{\lambda}_{\mathrm{em}}(t)$ for such aggregates mainly depends on two factors:

(*i*) The orientation of the phase director in the laboratory frame and the degree of order of the nematic phase.

(*ii*) The degree of order of the fluorophore in the local environment inside the micelles and its orientational dynamics, expressed by orientational correlation functions depending on second and fourth rank order parameters.

We have followed the formalism introduced by Zannoni [17] in order to obtain a form of $I^{\lambda}_{\mathrm{em}}(t)$ that is as general as possible, where these factors are explicitly taken into account. As a starting point we have

$$I_{\mathrm{if}}(t)=\left\langle\left(\sum_{L,m} E_{\mathrm{i}}^{*L,m} A_{\mathrm{Lab}}^{L,m}(\omega_0)\right)\left(\sum_{L',m'} E_{\mathrm{f}}^{*L',m'} \bar{A}_{\mathrm{Lab}}^{L',m'}(\omega_t)\right)\right\rangle P(t), \tag{3}$$

where $P(t)$ is the isotropic fluorescence decay. The two multiplying factors are the probability of absorption and emission of light, respectively, in the anisotropic phase; the labels i and f refer to the polarization axes of the incident and emitted light, respectively. **E** and **A** are second rank spherical tensors; the former describes the orientation of the polarizers, and the latter the orientation of the transition moments, both referred to the laboratory frame. The components of **E** are reported in table 1. The transition moment vectors, of course, are defined in a molecular reference frame, where the components of tensor **A** can be straightforwardly computed (see table 1). The averaging operation is performed on the molecular motion.

In order to relate the components of **A** in the molecular axis system to those in the laboratory frame, a series of intermediate frames has been introduced, with the Z axis lying on the local director inside the micelle, on the symmetry axis of the micelle and on

Table 1. Spherical components of tensor **E** in terms of its cartesian components and values assumed for particular orientations of vector **e**.

Cartesian components of vector **e**	$\parallel$	$\perp(y)$	$\perp(x)$
e_x, e_y, e_z	0,0,1	0,1,0	1,0,0
Spherical components of tensor **E** $E_{ij}=e_ie_j$			
$E^{0,0}=-\frac{1}{\sqrt{3}}(E_{11}+E_{22}+E_{33})$	$\frac{-1}{\sqrt{3}}$	$\frac{-1}{\sqrt{3}}$	$\frac{-1}{\sqrt{3}}$
$E^{2,0}=\sqrt{\frac{2}{3}}\left[E_{33}-\frac{(E_{11}+E_{22})}{2}\right]$	$\sqrt{\frac{2}{3}}$	$\frac{-1}{\sqrt{6}}$	$\frac{-1}{\sqrt{6}}$
$E^{2,\pm 1}=\mp[E_{13}\pm iE_{23}]$	0	0	0
$E^{2,\pm 2}=\frac{1}{2}[E_{11}-E_{22}\pm iE_{12}]$	0	$-\frac{1}{2}$	$\frac{1}{2}$

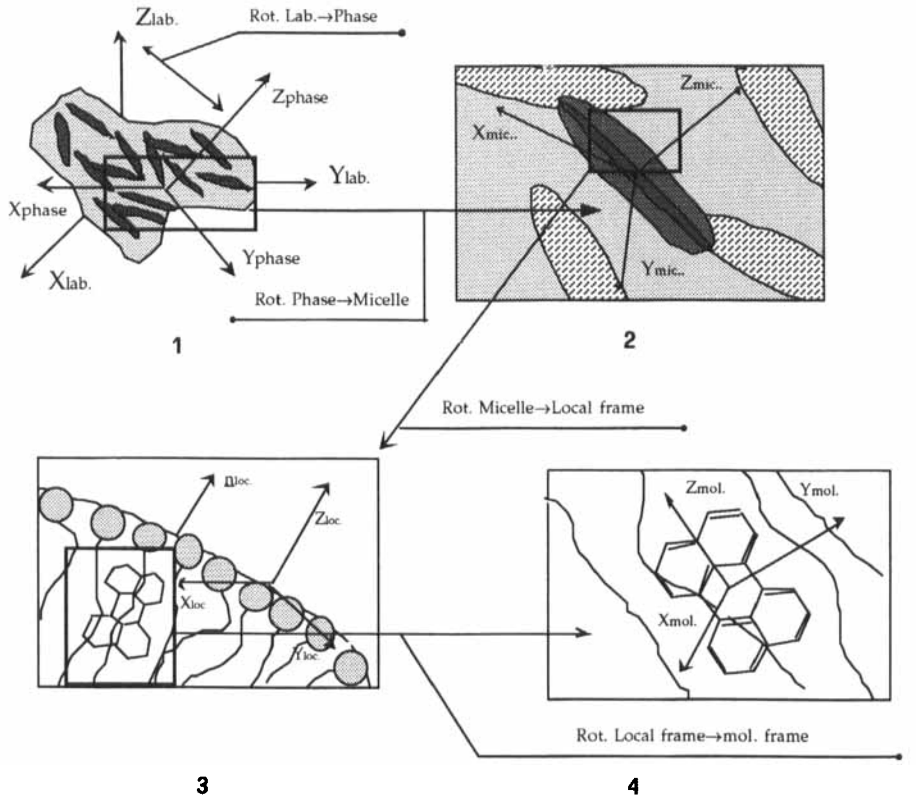

Figure 3. Visual representation of the intermediate rotations connecting the laboratory frame to the molecular frame expressed by equations (4 *a*)–(4 *d*). The passage through intermediate frames allows the separation of various contributions to the FD. (1) Phase director position with respect to the laboratory frame. (2) Micelle orientation relative to the phase director. (3) Local director distribution. (4) Fluorophore orientation in a local environment.

the phase director, respectively. The following transformations connect the tensor components in the various axis systems (see figure 3):

$$A^{L,m}_{\rm Lab} = \sum_{q_1} D^{*L}_{m,q_1}(\alpha_1,\beta_1,\gamma_1) A^{L,q_1}_{\rm Phase}, \tag{4 a}$$

$$A^{L,q_1}_{\rm Phase} = \sum_{q_2} D^{*L}_{q_1,q_2}(\alpha_2,\beta_2,\gamma_2) A^{L,q_2}_{\rm Mic}, \tag{4 b}$$

$$A^{L,q_2}_{\rm Mic} = \sum_{q_3} D^{*L}_{q_2,q_3}(\alpha_3,\beta_3,\gamma_3) A^{L,q_3}_{\rm Loc}, \tag{4 c}$$

$$A^{L,q_3}_{\rm Loc} = \sum_{q} D^{*L}_{q_3,q}(\alpha,\beta,\gamma) A^{L,q}_{\rm Mol}, \tag{4 d}$$

where α,β,γ are Euler angles and $D^{*L}_{q,q'}$ (α,β,γ) are Wigner rotation matrices. The cylindrical symmetry about the phase director, the micellar symmetry axis and the local director inside the micelle gives rise to the condition

$$q_1 = q_2 = q_3 = 0. \tag{5}$$

The sums in expression (4 *a*)–(4 *c*) are thereby reduced to single terms. The functions $D^{*L}_{m,0}(\alpha_1,\beta_1)$ describe the orientation of the phase director in the laboratory frame and their value is easily computed for the particular experimental setting adopted. The term $D^{*L}_{0,0}(\beta_3)$ (indicated in a shorter form by F^L) describes the orientation of the local director with respect to the micellar symmetry axis Z_{Mic}; it can assume different values in different regions of a typical aggregate [18]. In particular, $F^L=1$ for the approximately lamellar regions of a discotic aggregate where $\mathbf{n}_{\mathrm{Loc}} \| \mathbf{Z}_{\mathrm{Mic}}$ and $F^L=-\frac{1}{2}$ along a cylindrical aggregate where $\mathbf{n}_{\mathrm{Loc}} \perp \mathbf{Z}_{\mathrm{Mic}}$. We have assumed $F^L=1$. In this way, the discotic aggregates have been dealt with as lammellae; this approximation is adequate in the case of large aggregates, where the flat surface portion prevails. It must also be remembered that the solute itself might distribute and orient differently in regions with different curvature of the surface [19]. The possibility of such a complication has been neglected in the present work.

After performing the due substitutions and rearrangements (equation (4 *d*) is inserted into (4 *c*), and so on, then the resulting expression for $\mathbf{A}^{L,m}_{\mathrm{Lab}}$ is inserted into equation (3)), we can face the problem of the averaging on molecular motions. This operation involves the Wigner rotation matrices from equations (4 *b*) and (4 *d*) which are functions of angles variable with the molecular or micellar motion, and which are therefore functions of time. We obtain

$$I_{\mathrm{if}}(t)=\sum_{L,L'}\sum_{m,m'}E_{\mathrm{i}}^{L,m}E_{\mathrm{f}}^{L',m'}G^{L,L'}_{m,m'}(\alpha_1,\beta_1)F^LF^{L'\,\mathrm{Mic}}\varphi^{L,L'}(t)\sum_{q,q'}{}^{\mathrm{Mol}}\varphi^{L,L'}_{q,q'}(t)A^{L,q}_{\mathrm{Mol}}\bar{A}^{L',q'}_{\mathrm{Mol}}, \quad (6)$$

where $G^{L,L'}_{m,m'}=D^L_{m,0}(\alpha_1,\beta_1)D^{L'}_{m',0}(\alpha_1,\beta_1)$. These factors, as mentioned above, describe the orientation of the phase director in the laboratory frame. The definitions of the orientational correlation functions for the micelles, ${}^{\mathrm{Mic}}\phi^{L,L'}_{0,0}(t)$, and for the fluorescent molecule, ${}^{\mathrm{Mol}}\varphi^{L,L'}_{q,q'}(t)$, are the following:

$${}^{\mathrm{Mic}}\varphi^{0,0}_{0,0}(t)=\langle d^0_{0,0}(\beta_2^{(0)})d^0_{0,0}(\beta_2^{(t)})\rangle=1, \quad (7\,a)$$

$${}^{\mathrm{Mic}}\varphi^{0,2}(t)=\langle d^0_{0,0}(\beta_2^{(0)})d^2_{0,0}(\beta_2^{(t)})\rangle=\langle P_2^{\mathrm{Mic}}(t)\rangle, \quad (7\,b)$$

$${}^{\mathrm{Mic}}\varphi^{2,0}(t)=\langle d^2_{0,0}(\beta_2^{(0)})d^0_{0,0}(\beta_2^{(t)})\rangle=\langle P_2^{\mathrm{Mic}}(0)\rangle, \quad (7\,c)$$

$${}^{\mathrm{Mic}}\varphi^{2,2}(t)=\langle d^2_{0,0}(\beta_2^{(0)})d^2_{0,0}(\beta_2^{(t)})\rangle, \quad (7\,d)$$

$${}^{\mathrm{Mol}}\varphi^{0,0}_{0,0}(t)=\langle D^0_{0,0}(\omega_0)D^0_{0,0}(\omega_t)\rangle=1, \quad (7\,e)$$

$${}^{\mathrm{Mol}}\varphi^{0,2}_{0,q'}(t)=\langle D^{*2}_{0,q'}(\omega_t)\rangle, \quad (7\,f)$$

$${}^{\mathrm{Mol}}\varphi^{2,0}_{q,0}(t)=\langle D^{*2}_{0,q}(\omega_0)\rangle, \quad (7\,g)$$

$${}^{\mathrm{Mol}}\varphi^{2,2}_{q,q'}(t)=[\langle D^{*2}_{0,q}(\omega_0)D^{*2}_{0,q'}(\omega_t)\rangle], \quad (7\,h)$$

where ω_0 indicates the Euler angles β,γ at time 0, ω_t the same angles at time t. The integration of equations (7 *b*) and (7 *f*) is performed utilizing the joint orientation distribution function $P(\beta_2^{(0)}, \omega_0; \beta_2^{(t)}, \omega_t)$ for the micelle and the fluorophore. This distribution becomes $P(\beta_2^{(0)}, \omega_0)$ and $P(\beta_2^{(t)}, \omega_t)$ after integration over $\beta_2^{(t)}, \omega_t$ and $\beta_2^{(0)}, \omega_0$, respectively. If the micelle and fluorophore motions are independent, after integration on ω_0 and ω_t, we obtain $\langle P_2^{\mathrm{Mic}}(0)\rangle=\langle P_2^{\mathrm{Mic}}(t)\rangle$ and, after integration on $\beta_2^{(0)}$ and $\beta_2^{(t)}$, $P(\omega_0)$ and $P(\omega_t)$. These last functions represent the distribution functions for the fluorophore in the ground and excited state, respectively. For perylene we have assumed that these two functions are the same [22]

$$\langle D^{*2}_{0,q}(\omega_0)\rangle=\langle D^{*2}_{0,q}\rangle^{\mathrm{gr}}=\langle D^{*2}_{0,q}\rangle^{\mathrm{ex}}=\langle D^{*2}_{0,q}(\omega_t)\rangle, \quad (8\,a)$$

$\langle P_2^{\mathrm{Mic}}(t)\rangle$ and $\langle D^{*2}_{0,q}(\omega_t)\rangle$ are second rank order parameters of the nematic phase and of the probe molecule inside the micelle, respectively. If the motion of the micellar aggregates is slow with respect to that of the fluorophore inside the micelle, we can state

$$^{\mathrm{Mic}}\varphi^{2,2}(t)\approx\langle[d^2_{0,0}(\beta_2^{(0)})]^2\rangle=\langle[P_2^{\mathrm{Mic}}]^2\rangle. \tag{8 b}$$

According to a 'strong collision model' [9] the orientational correlation function of the fluorophore is described by a mono-exponential decay characterized by the rotational correlation time $\Theta_R^{q,q'}$. This hypothesis leads to the expression

$$\begin{aligned}^{\mathrm{Mol}}\varphi^{2,2}_{q,q'}(t)=&[\langle D^{*2}_{0,q}(\omega_0)D^{*2}_{0,q'}(\omega_0)\rangle-\langle D^{*2}_{0,q}(\omega_\infty)\rangle\langle D^{*2}_{0,q'}(\omega_\infty)\rangle]\\&\times\exp(-t/\Theta_R^{q,q'})+\langle D^{*2}_{0,q}(\omega_\infty)\rangle\langle D^{*2}_{0,q'}(\omega_\infty)\rangle.\end{aligned} \tag{8 c}$$

In our case, as we will see later, only the correlation function with $q=q'=0$ will survive. The correlation function $^{\mathrm{Mol}}\varphi^{2,2}_{0,0}(t)$ can be related to the fourth rank order parameters by the following expression [9]:

$$\langle D^{*2}_{0,0}(\omega_0)D^{*2}_{0,0}(\omega_0)\rangle=\tfrac{18}{35}\langle D^{*4}_{0,0}(\omega_0)\rangle+\tfrac{10}{35}\langle D^{*2}_{0,0}(\omega_0)\rangle+\tfrac{7}{35}.$$

We finally obtain for each spherical component of polarized emission (see table 1 for the **E** tensor)

$$I_{\parallel}^{0,0}=I_{\perp}^{0,0}=\tfrac{1}{9} \tag{9 a}$$

$$I_{\parallel}^{0,2}=\tfrac{1}{3}\sqrt{\tfrac{2}{3}}F^2G^{0,2}_{0,0}\,{}^{\mathrm{Mic}}\varphi^{0,2}(t)\sum_{q'}{}^{\mathrm{Mol}}\varphi^{0,2}_{0,q'}(t)\bar{A}^{2,q'}_{\mathrm{Mol}} \tag{9 b}$$

$$I_{\perp}^{0,2}=\tfrac{1}{3}F^2[\tfrac{1}{2}(G^{0,2}_{0,-2}+G^{0,2}_{0,2})]^{\mathrm{Mic}}\varphi^{0,2}(t)\sum_{q'}{}^{\mathrm{Mol}}\varphi^{0,2}_{0,q'}(t)\bar{A}^{2,q'}_{\mathrm{Mol}} \tag{9 c}$$

$$I_{\parallel}^{2,0}=I_{\perp}^{2,0}=\tfrac{1}{3}\sqrt{\tfrac{2}{3}}F^2G^{2,0}_{0,0}\,{}^{\mathrm{Mic}}\varphi^{2,0}(t)\sum_{q}{}^{\mathrm{Mol}}\varphi^{2,0}_{q,0}(t)A^{2,q}_{\mathrm{Mol}} \tag{9 d}$$

$$I_{\parallel}^{2,2}=\tfrac{2}{3}(F^2)^2G^{2,2}_{0,0}{}^{\mathrm{Mic}}\varphi^{2,2}(t)\sum_{q,q'}{}^{\mathrm{Mol}}\varphi^{2,2}_{q,q'}(t)A^{2,q}_{\mathrm{Mol}}\bar{A}^{2,q'}_{\mathrm{Mol}} \tag{9 e}$$

$$I_{\perp}^{2,2}=\sqrt{\tfrac{2}{3}}(F^2)^2[\tfrac{1}{2}(G^{2,2}_{0,-2}+G^{2,2}_{0,2})-\sqrt{\tfrac{1}{6}}G^{2,2}_{0,0}]^{\mathrm{Mic}}\varphi^{2,2}(t)\sum_{q,q'}{}^{\mathrm{Mol}}\varphi^{2,2}_{q,q'}(t)A^{2,q}_{\mathrm{Mol}}\bar{A}^{2,q'}_{\mathrm{Mol}}. \tag{9 f}$$

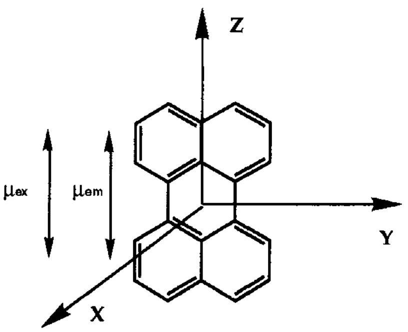

Figure 4. Molecular axis frame for perylene: the absorption and emission transition moments between the singlet S_0 and S_1 states are parallel to the Z_{mol} axis.

The molecular frame for perylene has the Z axis lying along the absorption transition moment, that is parallel also to the emission transition moment for the 409 nm transition (figure 4). This choice of the Z axis gives non-zero terms only for the $A_{\mathrm{Mol}}^{0,0}$ and $A_{\mathrm{Mol}}^{2,0}$ components of the **A** tensor. All contributions to the fluorescence depolarization which depend on biaxial order parameters ($\langle D_{0,\pm 2}^{2}\rangle$) vanish and we obtain information only on the $\langle D_{00}^{2}\rangle$ and $\langle D_{00}^{4}\rangle$ molecular order parameters. In fact, since information about order biaxiality is not contained in any of the components $I^{L,L'}$, no choice of the molecular frame can lead to the determination of independent values of $\langle D_{0,0}^{2}\rangle$ and $\langle D_{0,\pm 2}^{2}\rangle$.

The fluorescence lifetime of perylene, characterizing the function $P(t)$ of equation (3), was previously measured in a separate experiment. Perylene emission is described by a single lifetime corresponding to $t_{\mathrm{f}}=5{\cdot}6\pm 0{\cdot}3$ ns.

The cuvette setting corresponds to Euler angles $\alpha_1=30°$ and $\beta_1=90°$ (γ_1 is not an influence). We obtain for $I_{\|}$ and $I_{\perp}$

$$I_{\|}=\tfrac{1}{9}[1-2\langle P_2^{\mathrm{Mic}}\rangle\langle D_{00}^{2}\rangle+\langle(P_2^{\mathrm{Mic}})^2\rangle[\langle D_{00}^{2}\rangle^2+(\tfrac{18}{35}\langle D_{00}^{4}\rangle$$
$$+\tfrac{10}{35}\langle D_{00}^{2}\rangle-\langle D_{00}^{2}\rangle^2+\tfrac{7}{35})\exp(-t/\Theta_{\mathrm{R}})]]\exp(-t/\tau_{\mathrm{F}}), \tag{10a}$$

$$I_{\perp}=\tfrac{1}{9}[1-\tfrac{1}{4}\langle P_2^{\mathrm{Mic}}\rangle\langle D_{00}^{2}\rangle+\tfrac{-5}{4}\langle(P_2^{\mathrm{Mic}})^2\rangle[\langle D_{00}^{2}\rangle^2+(\tfrac{18}{35}\langle D_{00}^{4}\rangle$$
$$+\tfrac{10}{35}\langle D_{00}^{2}\rangle-\langle D_{00}^{2}\rangle^2+\tfrac{7}{35})\exp(-t/\Theta_{\mathrm{R}})]]\exp(-t/\tau_{\mathrm{F}}). \tag{10b}$$

For our calculations, we have used the simplest form for the micellar correlation functions: ${}^{\mathrm{Mic}}\varphi^{2,2}(t)={}^{\mathrm{Mic}}\varphi^{0,2}(t)=1$. This assumption transfers all the information on the micellar fluctuation to the parameters $\langle D_{00}^{2}\rangle$ and $\langle D_{00}^{4}\rangle$. In other words, what we determine are molecular order parameters relative to the phase director for a discotic phase and relative to an axis perpendicular to the phase director for a calamitic sample. The same kind of information is carried by the second rank order parameter $\langle D_{00}^{2}\rangle_{\mathrm{exp}}$ determined via ^{2}H NMR; therefore a direct comparison of the data obtained with the two techniques is possible. In a first approximation, the experimental second order parameter could be analysed as $\langle D_{00}^{2}\rangle_{\mathrm{exp}}\approx\langle D_{00}^{2}\rangle_{\mathrm{Mol}}\langle P_2\rangle_{\mathrm{Mic}}$.

The expressions of $I_{\|}$ and $I_{\perp}$, containing $\langle D_{00}^{2}\rangle$, $\langle D_{00}^{4}\rangle$ and Θ_{R} as variable parameters, were introduced in a computer routine for the numerical computation of the phase and modulation ratios at the experimental modulation frequencies (10–210 MHz). The experimental values were fitted using a non-linear least squares analysis program kindly supplied by Dr R. Ambrosetti (I.C.Q.E.M., Pisa). In figure 5 (*a*), an example of data fitting is shown. The resulting fitting parameters for perylene at various temperatures (T= 10, 20, 30, 40 and 50°C) are reported in table 2 and figures 5(*b*)–(*d*). The $\langle D_{00}^{2}\rangle$ values obtained by ^{2}H NMR in the same phase [6] are also reported.

4. Discussion

The aim of this work was to compare the data for the orientational order which can be extracted for the same phase with two completely different experimental techniques, i.e. fluorescence depolarization (FD) and deuterium nuclear magnetic resonance (^{2}H NMR).

The two sets of $\langle D_{00}^{2}\rangle$ data (the Z molecular axis defined in the present work corresponds to the Y axis of the ^{2}H NMR study) are in good agreement, within experimental error, for temperatures below 50°C, although the methods used for maintaining the macroscopic alignment of the sample are different (orienting effect of

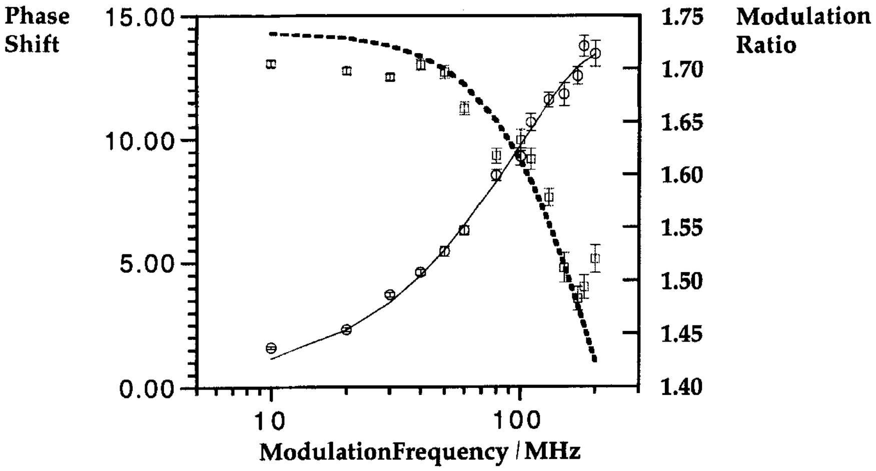
Phase Shift
15.00
10.00
5.00
0.00
1.75
1.70
1.65
1.60
1.55
1.50
1.45
1.40
Modulation Ratio
10
100
ModulationFrequency / MHz

(*a*)

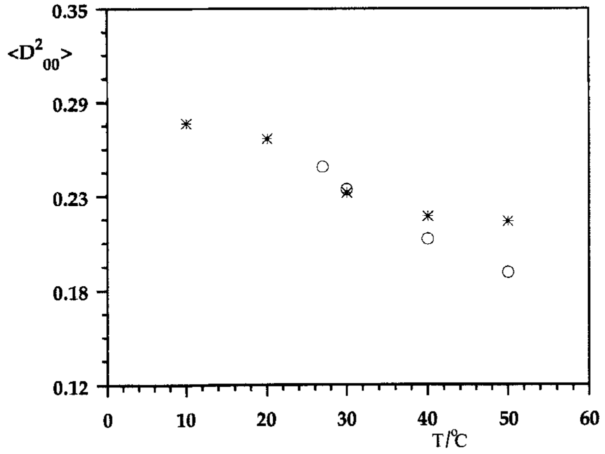
0.35
$\langle D^2_{00} \rangle$
0.29
0.23
0.18
0.12
0
10
20
30
40
50
60
T/°C

(*b*)

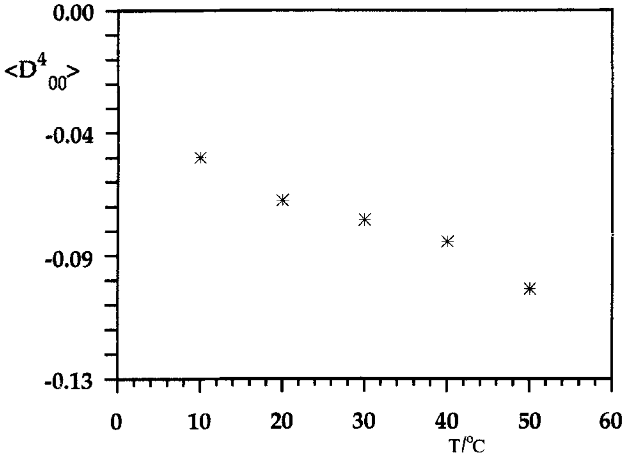
0.00
$\langle D^4_{00} \rangle$
-0.04
-0.09
-0.13
0
10
20
30
40
50
60
T/°C

(*c*)

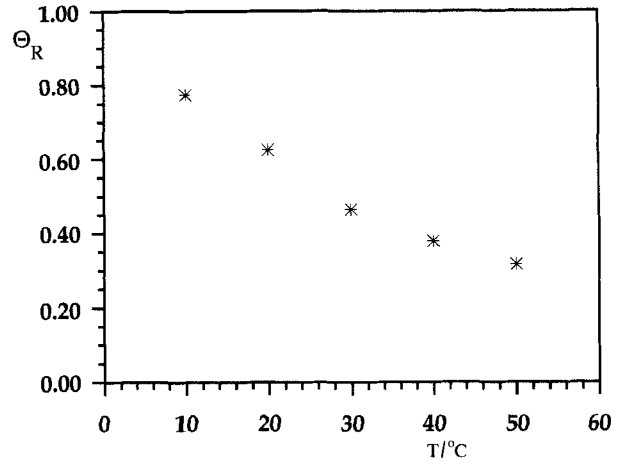

(*d*)

Figure 5. (*a*) Experimental phase shift (○) and modulation ratio (□) for perylene in the N_dII phase at $T=10°C$ versus the modulation frequency of the incident light. Computed trends of the phase shift (——) and modulation ratio (– – –). (*b*) Second rank order parameter $\langle D^2_{00}\rangle$ of perylene as a function of temperature: (*) FD data, (○) ^2H NMR results [6], (*c*) Fourth rank order parameter $\langle D^4_{00}\rangle$ and (*d*) orientational correlation time Θ_R of perylene versus temperature.

Table 2. Rotational correlation time and order parameters of perylene in the N_d II lyotropic phase.

Phase and method	T/°C	θ_R(ns)$\pm\sigma\theta_R$	$\langle D^2_{00}\rangle\pm\sigma\langle D^2_{00}\rangle$	$\langle D^4_{00}\rangle\pm\sigma\langle D^2_{00}\rangle$	$\mathrm{pol_S}$‡
N_dII/perylene fluorescence†	10	0·77±0·04	0·280±0·032	−0·052±0·005	−0·258
	20	0·62±0·02	0·270±0·018	−0·067±0·006	−0·260
	30	0·46±0·04	0·237±0·024	−0·074±0·018	−0·226
	40	0·38±0·05	0·222±0·027	−0·082±0·032	−0·218
	50	0·32±0·04	0·219±0·014	−0·098±0·030	−0·221
N_dII/perylene-d_{12} ^2H NMR§	31		0·239		
	39		0·209		
	51		0·188		

† $\tau_F=(5{\cdot}6\pm0{\cdot}2)$ns.
‡ Static polarization. The experimental uncertainty is about 0·001.
§ See [6].

cuvette surface for FD and magnetic field for ^2H NMR). The values of $\langle D^4_{00}\rangle$ and Θ_R reported in figure 5 follow a regular trend in the range of temperatures from $T=10$–40°C. An appreciable difference between the value of $\langle D^2_{00}\rangle$ from FD and ^2H NMR is observed at 50°C (the value of $\langle D^4_{00}\rangle$ at 50°C also deviates from the trend shown at lower temperatures). This could be explained considering that, with increasing the temperature and approaching the phase transition, which has been observed at 63°C for this phase [6, 10], inhomogeneities in the alignment of the sample could start to be important.

Let us now discuss the fourth rank order parameter $\langle D^4_{00}\rangle$. Usually, FD data are reported in terms of the decay time of the fluorescence anisotropy $r(t)$ and its limiting

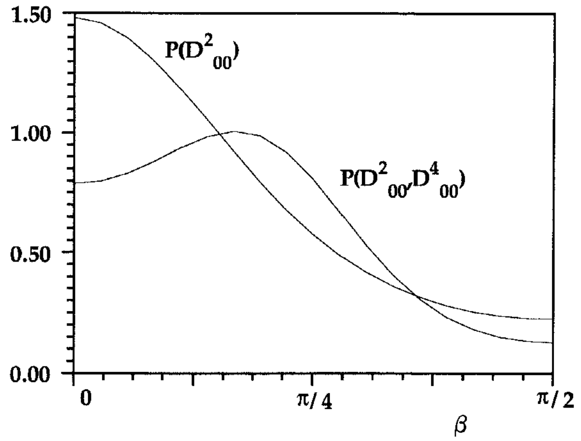

Figure 6. Orientational distribution functions obtained according to a maximum entropy approach. The probability $P(D^2_{00})$ values are expressed by a normalized distribution of the type $P(\beta) = N \exp[\lambda^2_{00} D^2_{00}{}^{(\beta)}]$ with $\lambda^2_{00} = 1{\cdot}258$. The $P(D^2_{00}, D^4_{00})$ function has the form $P(\beta) = N \exp[\lambda^2_{00} D^2_{00}{}^{(\beta)} + \lambda^4_{00} D^4_{00}{}^{(\beta)}]$ with $\lambda^2_{00} = 1{\cdot}572$ and $\lambda^4_{00} = -0{\cdot}857$. The λ values are derived by fitting the experimental order parameters from FD measurements at 10°C.

value $r(\infty)$. This fact makes difficult the comparison of our data with those of other authors, since $\langle D^4_{00} \rangle$ is normally not explicitly reported. It is perhaps useful to recall that this parameter is mainly determined by the initial value of the fluorescence anisotropy decay r_0, which can seldom be precisely detected. However, a small negative value of $\langle D^4_{00} \rangle$ is reported at least in one case [20].

According to a maximum entropy approach [21], we can use the values of $\langle D^2_{00} \rangle$ or both $\langle D^2_{00} \rangle$ and $\langle D^4_{00} \rangle$ to calculate the orientational distribution function for the Z axis of the molecule. The functions obtained from the order parameters at 10°C are shown in figure 6. The two distributions are substantially different. In particular, the latter shows a broad peak around 30°: in effect, a distribution peaked around 30° is what we could qualitatively expect from a small negative value of $\langle D^4_{00} \rangle$ in conjunction with a positive $\langle D^2_{00} \rangle$.

To date, no FD experiment has been reported in this type of lyotropic phase, which, on the other hand, has often been used as an orienting matrix for NMR structural studies [10]. Therefore, a comparison of our Θ_R is only possible with the values obtained for perylene in a N_cI phase based on K laurate [22]. Orientational correlation times found in this work are slightly lower than those measured for the cylindric phase. This indicates a lower micro-viscosity of the alkyl portion of the bilayers in N_dII phases than for the inner portion of the rod-like aggregates in the N_cI phase.

References

[1] Zager, S. A., and Freed, J. H., 1984, *Chem. Phys. Lett.*, **109**, 270.

[2] Johansson, L. B. A., and Lindblom, G., 1980, *Q. Rev. Biophys*, **13**, 63.

[3] Lakowicz, J. R., Prendergast, F. G., and Hogen, D., 1979, *Biochemistry*, **18**, 58.

[4] Johansson, L. B. A., and Lindblom, G., 1986, *Liq. Crystals*, **1**, 53.

[5] Emsley, J. W. (editor), 1983, *Nuclear Magnetic Resonance of Liquid Crystals* (NATO ASI Series, Vol. 141).

[6] Catalano, D., Corrado, A., Veracini, C. A., Shilstone, G. N., and Zannoni, C., 1979, *Liq. Crystals*, **4**, 217.

[7] Weber, G., 1977, *J. chem. Phys.*, **66**, 4081.

[8] Michl, J., and Thulstrup, E. W., 1986, *Spectroscopy with Polarized Light* (VCH Publ.), p. 327.

[9] Zannoni, C., Arcioni, A., and Cavatorta, P., 1983, *Chem. Phys. Lipids*, **32,** 179.

[10] Long, Jr., R. C., 1973, *J. magn. Reson.*, **12,** 216. Long, Jr., R. C., and Goldstein, J. H., 1973, *Molec. Crystals liq. Crystals*, **23,** 137; 1976, *J. magn. Reson.*, **23,** 523.

[11] Boonbrahm, P., and Saupe, A., 1984, *Molec. Crystals liq. Crystals* **109,** 225.

[12] Zinsli, P. E., 1977, *Chem. Phys.*, **20,** 299.

[13] Lakovicz, J. R., Cherek, H., Maliwal, B. P., and Gratton, E., 1985, *Biochemistry*, **24,** 376.

[14] Spencer, R. D., and Weber, G., 1970, *J. chem. Phys.*, **52,** 1654.

[15] Szabo, A., 1984, *J. chem. Phys.*, **81,** 150; 1980, *J. chem. Phys.*, **72,** 4620.

[16] Zannoni, C., 1979, *Molec. Phys.*, **38,** 1813; 1984, *Chem. Phys. Lett.*, **110,** 325.

[17] Arcioni, A., Tarroni, R., and Zannoni, C., 1988, *Polarized Spectroscopy of Ordered Systems*, edited by B. Samori and W. E. Thulstrup (Kluwer Academic Publishers).

[18] Carvolin, J., and Hendrikx, 1983, *Nuclear Magnetic Resonance of Liquid Crystals*, edited by J. W. Emsley (NATO ASI Series, Vol. 141), pp. 449–471.

[19] Fisz, J. J., 1989, *Chem. Phys.*, **132,** 303; 1989, *Chem. Phys.*, **132,** 315.

[20] Arcioni, A., Bertinelli, F., Tarroni, R., and Zannoni, C., 1990, *Chem. Phys.*, **143,** 259.

[21] Jaynes, E. T., 1957, *Phys. Rev.*, **106,** 620; Chiccoli, C., Pasini, P., Biscarini, F., and Zannoni, C., 1988, *Molec. Phys.*, **65,** 1505.

[22] Johansson, L. B. A., Molotkovsky, J. G., and Bergelson, L., 1987, *J. Am. chem. Soc.*, **109,** 7374. Johansson, L. B. A., 1990, *J. chem. Soc. Faraday Trans.*, **86,** 2103.